# Simulating Disordered Many-Body Open Quantum Systems: Modelling Organic Polariton Bose-Einstein Condensation

Joel Beckles
Supervisor: Dr. Jonathan Keeling

August 15, 2022

**Abstract**

The theory of open quantum systems allows for a realistic description of quantum phenomena by accounting for a system's interactions with its environment. Using this theory, computational methods were previously implemented in the OQuPy Python package to model a single open system. These methods were able to simulate the dynamics of many organic molecules of a single type transitioning into a state of matter known as Bose-Einstein Condensate. In this paper, these computational methods are expanded so that they can model multiple types of molecules undergoing condensation. Particular focus is given to the case of disorder, where different types of molecules have different energies.

## 1 Acknowledgements

I would like to especially thank Dr. Jonathan Keeling for allowing me to work on this project and for supervising me throughout my internship as well as Piper Fowler-Wright who has also provided a great deal of assistance in my understanding of the concepts and code related to this project. I would also like to extend gratitude to the Laidlaw Foundation for funding this project and to Lord Laidlaw himself for catalyzing this initiative.

## 2 Introduction

The study of quantum mechanics has managed to describe the microscopic world remarkably well. One often formulates problems in quantum mechanics by considering how physical systems, like molecules, evolve over time and by considering how they change when acted upon by external operations like measurement. However, there is always some interaction between systems of interest and other systems with which one is not concerned. An open quantum system may be defined as one which interacts with its environment. Strictly speaking, since no system is ever truly isolated from its surroundings, all quantum systems may be regarded as open. It is therefore useful to have a framework in which one considers there to be a (closed) "total system" which comprises open quantum systems of interest and their environments [1, 2].

There are cases in which the interaction between open systems and their environments is weak, or where such interaction only changes the environments over a short timescale relative to the open system dynamics. In such cases, quantum processes are generally well-described using Markovian models [3, 4]. A quantum process may be described as Markovian when, after measurement, the future state of a system depends only on its current state [5]. Markovian models are deemed "memoryless" as a system's environment at any given time is independent of any past interactions it had with the system.

Many real-world quantum systems do not exist in environments which satisfy the requirements of a Markovian model. The dynamics of such systems are referred to as non-Markovian. Non-Markovian environments carry "memory" associated with a system's previous states.

It is therefore desirable to find efficient methods which can incorporate all the information about a quantum system's state as it both evolves over time and undergoes measurement. This can have practical applications ranging from modelling fault-tolerant quantum devices to modelling complex biomolecular processes [6–8].

As will be discussed in more detail in section 4, the mathematical framework of tensor networks [9, 10] has proven to be an effective means of modelling the non-Markovian dynamics of open quantum systems. Many recent computational methods have been developed based on this framework [11–17].

One application of these methods is modelling organic molecules which interact strongly with light. When light is trapped in a microcavity with organic molecules, hybrid light-matter excitations known as polaritons can be formed. As will be discussed in further detail in section 3, under certain conditions, these polaritons can undergo a process known as Bose-Einstein condensation. In this case, the open systems are organic molecules, and the environment involves molecular vibration and external measurement.

The tensor-network-based computational methods implemented in Ref. [18] have so far been able to simulate the dynamics of a single type of system [14]. In this paper, we show that these methods have been expanded to simulate the dynamics of any number of system types, with particular focus on their application to polariton Bose-Einstein condensation for multiple types of molecules within a microcavity. The development of organic polariton simulation techniques has exciting potential applications in the fields of lasing, circuit-manufacturing, quantum computing, photophysics and organic chemistry [19, 20].

In section 3, we discuss the process of organic polariton Bose-Einstein Condensation, and explain how multiple types of molecules can now be modelled together. In section 4, we discuss how the tensor network framework is being used for efficient simulation of the dynamics of these multi-system models. In section 5, the results of the computational methods will be presented, including a look at the case where molecules are disordered. Finally, in section 6, the efficiency of the computational methods used will be evaluated.

## 3 Organic Polariton Bose-Einstein Condensation

When light travels through a solid, it induces, and is affected by, polarization within the material. This combination of light and polarized waves is quantized as it can only transfer energy in discrete amounts. A "quasiparticle"[1] possessing a quantum of such energy is known as a polariton [21]. There are three main types of polaritons: phonon-polaritons, plasmon-polaritons and exciton-polartions [22]. Exciton-polaritons will be the type discussed in this paper.

Excitons are electronic excitations which can be thought of as quasiparticles consisting of an electron and a (positive) hole[2] [23–25]. Exciton-polaritons occur when light provides the excitation required to create excitons within a material (see Figure 2). The type of excitons generally formed in organic molecules are known as Frenkel excitons. Frenkel excitons are highly localized [25, 26] and may transfer electronic excitations via hopping [27].

Bose-Einstein Condensate (BEC) may be defined as a state of matter in which a large (macroscopic) number of particles all occupy a single (ground-state) energy level. The particles, or quasiparticles, which occupy this level must be bosons, i.e. they must have integer spin. In the case of exciton-polariton condensates, excitons—which comprise two (half-integer) fermions—can be regarded as bosons [28]. BEC begins to form when the de Broglie wavelength[3] of particles becomes larger than the interparticle spacing. This de Broglie wavelength is inversely proportional to both particle mass and temperature [20, 27]. Exciton-polaritons trapped within a reflective microcavity (see Figures 1 and 2) can have very small effective masses (e.g. of the order of $10^{-4}$ times that of an electron [27, 28]), thereby allowing for the possibility of room-temperature condensate [27, 29].

In theory, polariton condensates are allowed to form at room temperature but warm temperatures become a practical challenge for many materials. The high binding energies and large oscillator strengths of Frenkel excitons in organic molecules make them well-suited for study of polariton condensation at room temperature [27, 30]. This is remarkable when compared to the $\sim 10K$ cryogenic temperatures required for other polariton BEC, and the even colder billionth of a degree above absolute zero required for traditional atomic gas BEC [31].

[1] By "quasiparticle", it is meant that, within the appropriate context, the disturbance within matter can be modelled as if it were a particle.

[2] More precisely, in the context of molecular excitation, an exciton is formed from the excitation of an electron from the highest occupied molecular orbital to the lowest unoccupied molecular orbital.

[3] The de Broglie wavelength is the wavelength associated with the wave-like behaviour of particles and is defined as $\lambda_{dB} = h/p$ where $h$ is Planck's constant and $p$ is the particle's momentum.

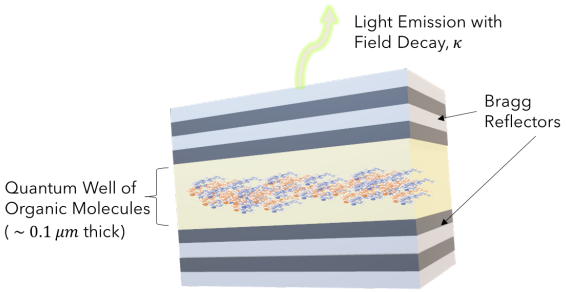


Figure 1: Diagram of reflective microcavity with organic molecules. Two types of systems (organic molecules) are depicted within a "quantum well", shown by orange and blue molecules. The molecules are excited, for instance by an external pump laser (not shown here). The excited molecules then emit light which is confined between two mirrors known as Bragg Reflectors. The reflected light is reabsorbed by the molecules, creating a cycle of emission and reabsorption.

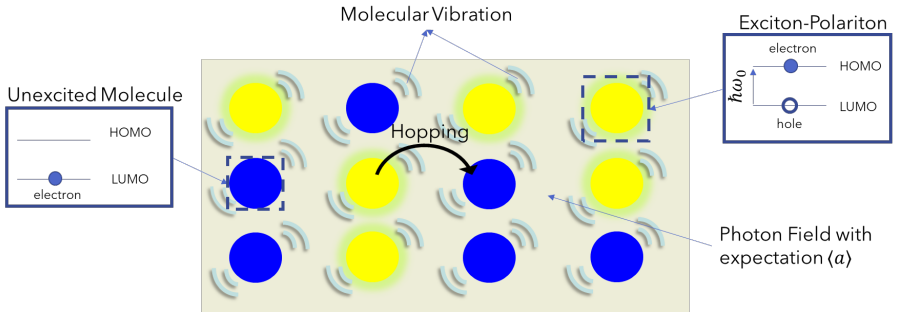


Figure 2: Simplified illustration of molecular excitation in the microcavity. A zoomed in section of the lattice of some blue molecules in Figure 1 is shown. The molecules are vibrating and are in the presence of the photon field confined in the microcavity. Light can excite an electron in a molecule from the Lowest Unoccupied Molecular Orbital (LUMO) to the Highest Occupied Molecular Orbital (HOMO). Excitations may hop from one place to another within the lattice.

It is computationally impractical to calculate the quantum non-Markovian dynamics of tens of thousands of molecules when trying to model organic microcavity polariton condensation. It is therefore appropriate to use an approach known as mean-field theory, in which the dynamics of each type of molecule can be reduced to a problem suitable for tensor-network-based computational methods [14]. Building on the work done in Ref. [14] which models the non-Markovian dynamics for a single type of molecule involved in polariton condensation, this paper shows how the dynamics of any number of molecule types can be simulated.

## 3.1 Mathematical Treatment of Multi-System Polariton Condensates

Using mean-field theory, it can be shown that the dynamics for many molecules of a single type are governed by a pair of coupled equations [14]. One of these equations is the mean-field Hamiltonian, which describes the energy of the system, while the other equation describes the rate of change of the field expectation[4] with respect to time (see equations 5 and 6 in Ref. [14]).

Code has now been written to model the dynamics of any number of open quantum systems. Applied to the problem of polariton condensates, this means that we can investigate the dynamics of multiple types of organic molecules within a microcavity, with there being possibly thousands of identical molecules of each type. This is now described by coupled equations consisting of different system Hamiltonians and a single equation of motion which evolves the field expectation over time. In the following equations, we note that we use natural units, thereby setting the reduced Planck constant, $\hbar = 1$.

[4]By "field" here, we are referring to the electromagnetic field associated with the light in the microcavity.

In this case, the Hamiltonian of a quantum system, $s$, in a list of quantum systems is

$$H_{MF,s} = \frac{\omega_{0,s}}{2}\sigma_s^z + \frac{g}{2}(\langle a\rangle\sigma_s^+ + \langle a\rangle\sigma_s^-) \tag{1}$$

where $\omega_{0,s}$ is the angular frequency associated with the excitation energy of a molecule, $\sigma_s^z$ is the Pauli matrix[5] corresponding to the measurement of the system's spin in the $z$-component of a Cartesian coordinate system, $g$ is the coupling strength between light and the molecules within the microcavity, $\langle a\rangle$ is the expectation value of the field, and $\sigma_s^+$ and $\sigma_s^-$ are the raising and lowering operators[6] for the system's spin respectively.

Secondly, the field equation of motion now takes a weighted sum of the states of each of the systems involved. For each type of system $s$, the state is weighted by the number of such molecules, $N_s$. Mathematically, the partial derivative of the field expectation with respect to time, $t$ is given by:

$$\partial_t\langle a\rangle = -(i\omega_c + \kappa)\langle a\rangle - i\frac{g}{2}\sum_s N_s\langle\sigma_s^-\rangle \tag{2}$$

where $\omega_c$ is the angular frequency of light resonant within the microcavity, $\kappa$ is the field decay constant (a measure of the rate at which light leaks out of the microcavity mirrors) and $\langle\sigma_s^-\rangle$ is the average of the identical spins in each type of system $s$.

The environment of the molecules at a given temperataure, $T$, may be described by considering the spectral density of the molecules involved. This is a measure of the energy absorption across a range of possible environmental frequencies, $\nu$, and can be written [14] as

$$J(\nu) = 2\alpha\nu e^{-(\nu/\nu_c)^2}, \qquad \nu > 0 \tag{3}$$

where $\alpha$ is the environmental coupling strength (i.e. a measure of how strong system-environment interactions are) and $\nu_c$ is the frequency at which maximum light absorption occurs (known as the cut-off frequency). Additionally, we also consider that there is some molecular dissipation of energy, $\Gamma_\downarrow$ (similar to $\kappa$)[7], and external pumping of energy into the system, $\Gamma_\uparrow$.

# 4 Discussion of Tensor Network Approach

Tensors are mathematical objects which generalize the concepts of scalars, vectors and matrices. The rank of a tensor is the number of dimensions required to describe it. For example, a rank-0 tensor is a scalar, a rank-1 tensor is a vector and a rank-2 tensor is a matrix. A mathematical formalism known as tensor networks has been developed using tensors to efficiently model a variety of problems involving many-body quantum systems [32, 33].

Tensor networks may be represented diagramatically by vertices and edges which we shall refer to as "legs". A rank-two tensor, for example, is represented by a vertex with two legs. Two tensors may undergo contraction with one another to produce a new tensor. For the case of a matrix contracted with a vector, this is the same as matrix-vector multiplication, the result of which is another vector. This is illustrated in Figure 3.

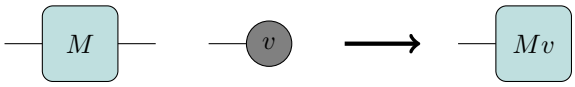


Figure 3: Illustration of tensor networks being used for matrix-vector calculation. A matrix, $M$, is contracted with a vector, $v$, resulting in another vector $Mv$. One can think of the contraction as the joining of the right leg of M with the (left) leg of $v$ to form a new single vertex.

Two relevant computational techniques which make use of this formalism are the Time Evolving Matrix Product Operator (TEMPO) [11], which can simulate the time-evolution of non-Markovian

[5] Mathematically, $\sigma^z = \begin{pmatrix} 1 & 0 \\ 0 & -1 \end{pmatrix}$

[6] Mathematically, $\sigma^+ = \begin{pmatrix} 0 & 1 \\ 0 & 0 \end{pmatrix}$ and $\sigma^- = \begin{pmatrix} 0 & 0 \\ 1 & 0 \end{pmatrix}$

[7] This energy loss is associated with processes like non-radiative energy loss or photon emission at non-resonant frequencies of light in the cavity.

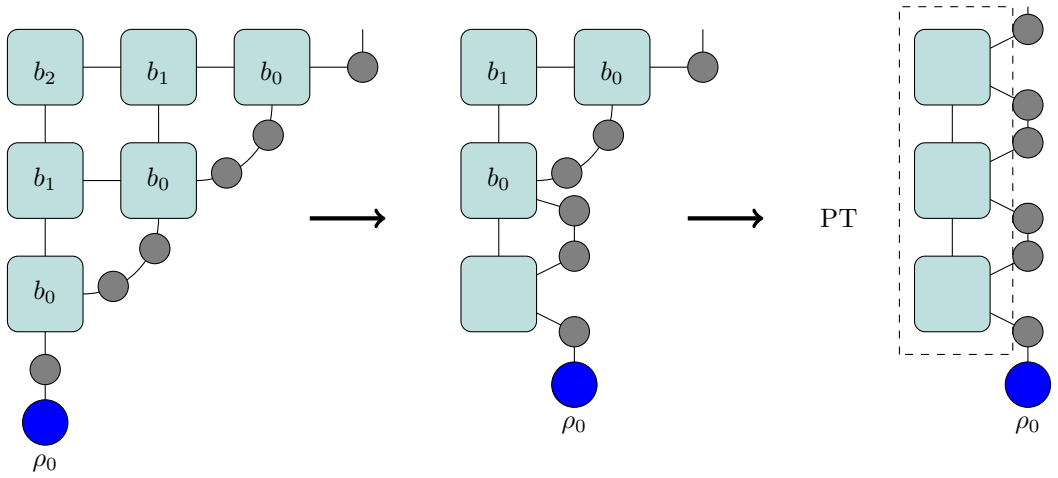


Figure 4: Horizontal contraction scheme for the constrcution of a Process Tensor (PT). The squares represent bath tensors, with $b_k$ being the $k$th bath tensor. The bath tensors encapsulate information about an open system's environment. Grey circles represent system propagators, which propagate the system forward in time. Note that the initial state $\rho_0$, and the system propagators are shown in the process tensor construction scheme only for illustrative purposes. In practice, process tensors are independently computed, allowing for use by different systems while saving computation time.

open quantum systems, and the process tensor (PT), which efficiently describes the environment of an open system [9]. The combination of these two techniques has birthed what is referred to as the Process Tensor Matrix Product Operator (PT-MPO) as implemented, for example, in Refs. [14] and [34].

Figure 4 illustrates how a process tensor representation of a quantum system's environment is constructed[8]. Figure 5 illustrates the contraction of a tensor network to determine a quantum system's state at a given time.

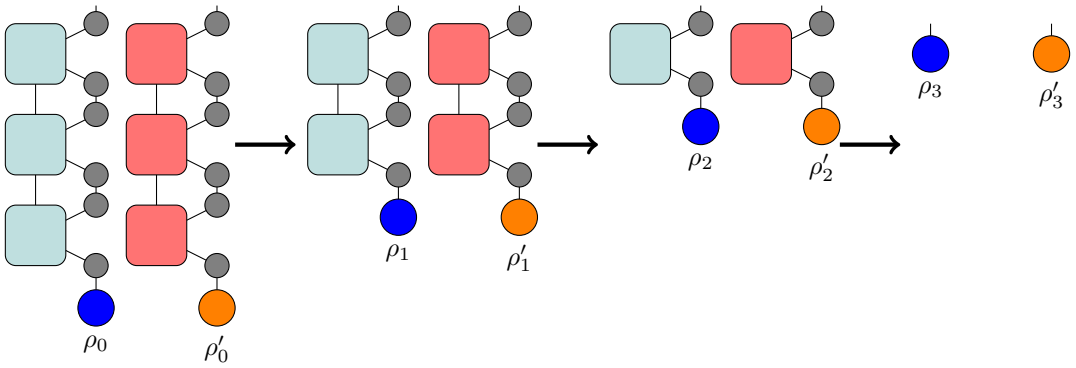


Figure 5: Illustration of multi-system contraction scheme for evolving quantum states over time. Time evolution takes place in the vertical direction. The states of two systems, $\rho_n$ and $\rho_n'$, are shown to evolve $n = 3$ time-steps forward. This depicts the most general case allowed by the code in which distinct systems have different process tensors (corresponding to different system environments). The final result is a state vector for both systems. Note that the system's state does not have to be calculated up to the final time-step of the process tensor. The code allows for contraction up to an intermediate time step as well.

[8]Though not technically depicted here, all bath tensors have the same rank. The bath tensor $b_2$ in Figure 4, for example, is shown to be of rank 2 when it is really of rank 4. This problem is remedied by the use of "sum caps" (see, for example, the tensor network depiction in [15]).

# 5 Testing and Results of Code

## 5.1 Single-system Dynamics Test

As a test for the reliability of the new code which was written, the dynamics for a single type of molecule was first simulated. This was done to ensure that the results obtained are consistent with those previously obtained in the single-system case by Ref. [14]. The microcavity organic molecule modelled is brominated boron dipyrromethene (BODIPY-Br) and all the relevant parameters for describing the system's dynamics are shown in Table 1.

| Parameters | Values | Units |
|---|---|---|
| $\omega_0$ | 0 | eV |
| $\omega_c$ | -0.02 | eV |
| $\alpha$ | 0.25 | dimensionless |
| $T$ | 300 | K |
| $\Gamma_\uparrow$ | 0.0125 | eV |
| $\Gamma_\downarrow$ | 0.01 | eV |
| $g$ | 0.2 | eV |
| $\nu_c$ | 0.15 | eV |
| $\kappa$ | 0.01 | eV |

Table 1: Table displaying parameters for single system-type dynamics test

The plot obtained in Figure 6 agrees exactly with the plot obtained by Ref. [14] for the same parameters (pump strength $\Gamma_\uparrow/\Gamma_\downarrow$ of 0.8). This suggests that the generalization of the previous code did not hamper its regular single-system-type calculations.

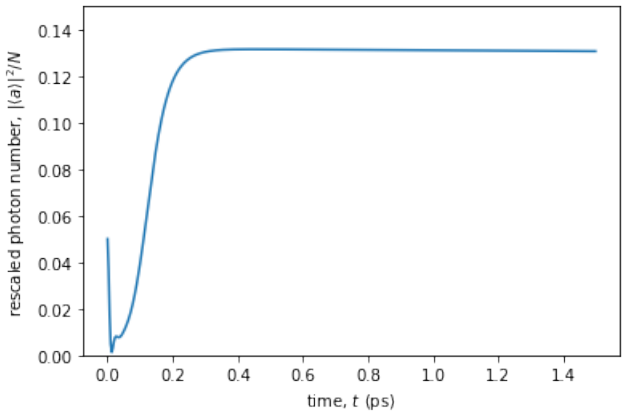


Figure 6: Plot of rescaled photon number ($|\langle a \rangle|^2/N$) against time ($t$) for a single system type, where $N$ is the total number of molecules across all systems

## 5.2 Spin Expectation of Different Systems coupled to a Field

In order to check whether new multi-system dynamics can be investigated using the code written, a simulation was run for two distinct systems coupled to a field. In order to test that the code can be as general as possible, both systems were given different process-tensor environments. The first system, system 0, had the same parameters as in Table 1, but with two different environments now - each with their own environmental coupling strength $\alpha$ (0.25 and 0.1). The second system, system 1, has the same parameters as in Table 1, except for the fact that it has one value of $\alpha = 0.9$. Figure 7 shows the results of this simulation.

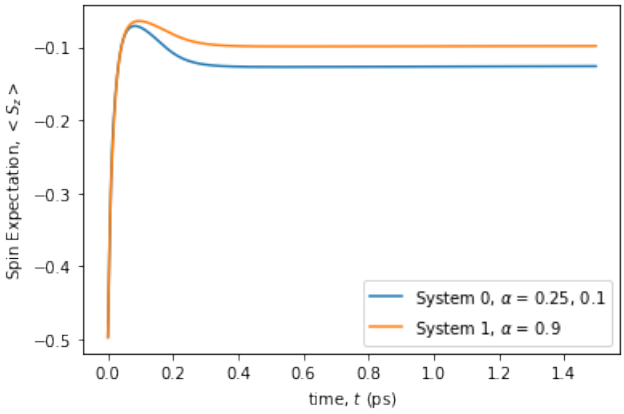


Figure 7: Plot of spin expectation ($\langle S_z \rangle$) against time ($t$) for two systems coupled to the same field

### 5.3 Disordered Mean Field Dynamics

A composite system may be considered disordered when its subsystems have different Hamiltonian equations, due for example to variations in their energies ($\hbar\omega_0$). The generalizations made by this code allow for simulation of composite systems coupled to a field, making disorder a natural topic to consider. To introduce disorder into a composite system, we used the inverse error function[9] to distribute values of $\omega_0$ across systems within the composite system such that the mean value of $\omega_0$ is zero. The remaining parameters for the systems are as detailed in Table 2.

| Parameters | Values | Units |
|---|---|---|
| $\omega_c$ | 0 | eV |
| $\alpha$ | 0.25 | dimensionless |
| $T$ | 300 | K |
| $\Gamma_\uparrow$ | 0.01 | eV |
| $\Gamma_\downarrow$ | 0.01 | eV |
| $g$ | 0.2 | eV |
| $\nu_c$ | 0.15 | eV |
| $\kappa$ | 0.01 | eV |

Table 2: Table displaying parameters for investigation of disorder

Figure 8 shows plots of photon number against time for composite systems with different levels of variance in the distribution of $\omega_0$ (with the number of systems in each composite system fixed at 10). It appears that increased disorder reduces the damped oscillations in photon number.

Figure 9 shows plots for composite systems with the same level of disorder ($\omega_0$ deviation $= 0.15eV$) but different numbers of subsystems. We note that, as one might expect, as the number of systems gets larger, the effects of disorder on the photon number converge.

## 6 Efficiency of Multi-system Computation

In order to check how computation time scaled with the number of systems being simulated, we timed a computation using the parameters in Table 1 for varying numbers of systems coupled to a field. Figure 10 shows a clear linear trend in runtime with system number, which is reasonably efficient when one considers that process tensors are computed beforehand for simulations and may be reused by several different systems.

[9]This is the inverse of the error function, $erf(x)$, which is defined as $erf(x) = \frac{2}{\sqrt{\pi}} \int_0^x e^{-t^2}\, dt$.

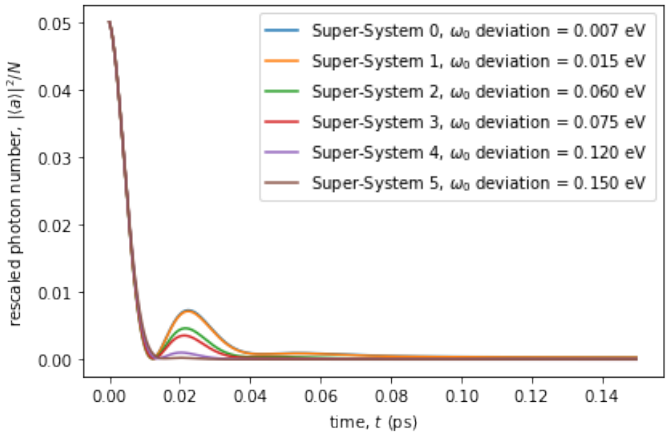


Figure 8: Plot of rescaled photon number ($|\langle a \rangle|^2/N$) against time ($t$) for different deviation values in $\omega_0$, and a fixed number of systems, 10. Here, "Super System" refers to a composite system containing miultiple unique quantum systems.

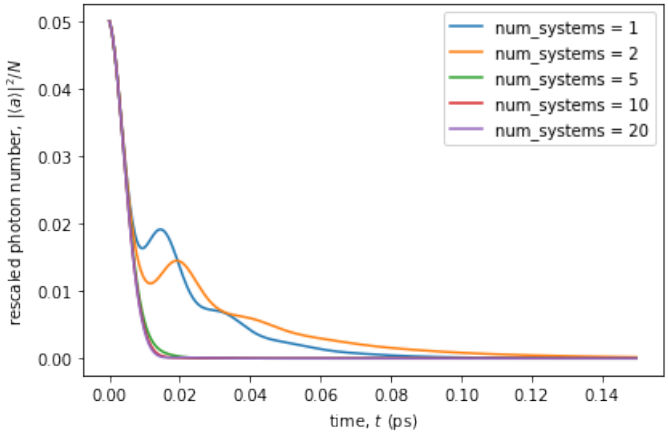


Figure 9: Plot of rescaled photon number ($|\langle a \rangle|^2/N$) against time ($t$) for a fixed deviation value of $\omega_0$ and different numbers of systems

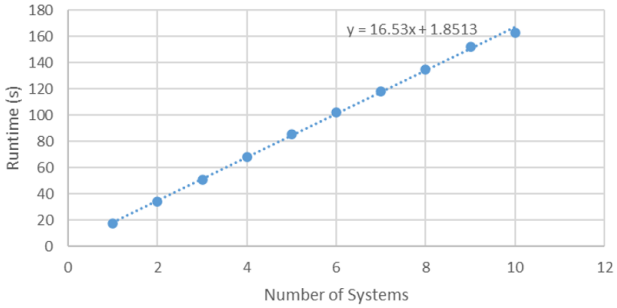


Figure 10: Plot of runtime against number of systems for computing field dynamics (with a pre-computed process tensor)

## 6.1 Brief Discussion on Potential Efficiency Improvements

In addition to the work described above, some more general programming efficiency considerations were made. Where possible, in generalising the code implemented in [18], unnecessary variable def-

initions were removed via the use of list comprehensions[10]. However, on its own, these changes are unlikely to have caused any significant runtime improvements. As this code involves many array-based calculations, in future, it may be worth being more strict about using only numpy [35] arrays instead of standard Python lists (except where absolutely necessary). This would maximize the benefits of numpy's efficient array-based calculations and allow for efficient compilation by a tool like numba [36].

# 7 Conclusion and Potential Applications of Work Done

It has been seen that the new code written has successfully been able to simulate the non-Markovian dynamics of open quantum systems, particularly in the case of models for polariton BEC. The case of disorder among composite molecular systems was investigated and it was observed that results for photon number converge as the number of coupled systems within a composite system increases. It was found that the runtime for these computations scaled linearly with the number of systems under investigation. In future, this code can be used to investigate many interesting physical phenomena within the field of polariton BEC and beyond. One such phenomenon is the energy exchange undergone between different types of molecules within a microcavity. To date, the new code written is available on GitHub at `https://github.com/JoelANB/OQuPy/tree/linearisation_fix`, but it is anticipated that these developments will be merged into the main OQuPy package.

# References


[1] D. Manzano, AIP Advances **10**, 025106 (2020).

[2] C.-F. Li, G.-C. Guo, and J. Piilo, EPL (Europhysics Letters) **127**, 50001 (2019).

[3] C. P. Koch, Journal of Physics: Condensed Matter **28**, 213001 (2016).

[4] H.-P. Breuer and F. Petruccione, *The theory of open quantum systems* (Oxford Scholarship Online, 2007).

[5] F. A. Pollock, C. Rodríguez-Rosario, T. Frauenheim, M. Paternostro, and K. Modi, Phys. Rev. Lett. **120**, 040405 (2018).

[6] D. Burgarth, P. Facchi, D. Lonigro, and K. Modi, Phys. Rev. A **104**, L050404 (2021).

[7] M. Thorwart, J. Eckel, J. Reina, P. Nalbach, and S. Weiss, Chemical Physics Letters **478**, 234 (2009).

[8] S. Milz and K. Modi, PRX Quantum **2**, 030201 (2021).

[9] F. A. Pollock, C. Rodríguez-Rosario, T. Frauenheim, M. Paternostro, and K. Modi, Phys. Rev. A **97**, 012127 (2018).

[10] A. Strathearn, "Results", in *Modelling non-markovian quantum systems using tensor networks* (Springer International Publishing, Cham, 2020), pp. 83–97.

[11] A. Strathearn, P. Kirton, D. Kilda, J. Keeling, and B. W. Lovett, Nature Communications **9**, 3322, 3322 (2018).

[12] M. R. Jørgensen and F. A. Pollock, Phys. Rev. Lett. **123**, 240602 (2019).

[13] G. E. Fux, E. P. Butler, P. R. Eastham, B. W. Lovett, and J. Keeling, Phys. Rev. Lett. **126**, 200401 (2021).

[14] P. Fowler-Wright, B. W. Lovett, and J. Keeling, arXiv:2112.09003 (2021).

[15] D. Gribben, A. Strathearn, G. E. Fux, P. Kirton, and B. W. Lovett, arXiv:2106.04212 (2021).

[16] D. Gribben, D. M. Rouse, J. Iles-Smith, A. Strathearn, H. Maguire, P. Kirton, A. Nazir, E. M. Gauger, and B. W. Lovett, PRX Quantum **3**, 010321 (2022).

[17] M. Cygorek, M. Cosacchi, A. Vagov, V. Axt, B. Lovett, J. Keeling, and E. Gauger, English, Nature Physics **18**, 662 (2022).

[18] The TEMPO collaboration, *OQuPy: A Python 3 package to efficiently compute non-Markovian open quantum systems*. GitHub, 2020.

[19] D. Sanvitto and S. Kéna-Cohen, Nature Materials **15**, 1061 (2016).

[20] Z. Jiang, A. Ren, Y. Ren, J. Yao, and Y. S. Zhao, Advanced Materials **34**, 2106095 (2022).


[10] List comprehensions are a syntactic shortcut available in the Python programming language which allows for efficient reuse of variables which have already been defined.

[21] C. F. Klingshirn, *Semiconductor optics* (Springer Berlin, Heidelberg, 2012).

[22] D. T. Ha, D. T. Thuy, V. T. Hoa, T. T. T. Van, and N. A. Viet, Journal of Physics: Conference Series **865**, 012007 (2017).

[23] S. Sanguinetti, M. Guzzi, E. Gatti, and M. Gurioli, in *Characterization of semiconductor heterostructures and nanostructures (second edition)*, edited by C. Lamberti and G. Agostini, Second Edition (Elsevier, Oxford, 2013), pp. 509–556.

[24] C. J. Bardeen, Annual Review of Physical Chemistry **65**, PMID: 24313684, 127 (2014).

[25] K. W. Böer and U. W. Pohl, "Excitons", in *Semiconductor physics* (Springer International Publishing, Cham, 2018), pp. 485–525.

[26] M. Combescot and S.-Y. Shiau, *Excitons and cooper pairs: two composite bosons in many-body physics* (Oxford Scholarship Online, 2015).

[27] J. Keeling and S. Kéna-Cohen, Annual Review of Physical Chemistry **71**, PMID: 32126177, 435 (2020).

[28] T. Byrnes, N. Y. Kim, and Y. Yamamoto, Nature Physics, 10.1038/nphys3143 (2014).

[29] N. Proukakis, D. Snoke, and P. Littlewood, eds., *Universal themes of bose-einstein condensation* (Cambridge University Press, 2017).

[30] S. Kéna-Cohen and S. R. Forrest, Nature Photonics **4**, 371 (2010).

[31] H. Deng, H. Haug, and Y. Yamamoto, Rev. Mod. Phys. **82**, 1489 (2010).

[32] R. Orús, Annals of Physics **349**, 117 (2014).

[33] R. Orús, Nature Reviews Physics, 10.1038/s42254-019-0086-7 (2019).

[34] G. E. Fux, D. Kilda, B. W. Lovett, and J. Keeling, arXiv:2201.05529 (2022).

[35] C. R. Harris, K. J. Millman, R. van der Walt Stéfan J.and Gommers, P. Virtanen, D. Cournapeau, E. Wieser, J. Taylor, S. Berg, N. J. Smith, R. Kern, M. Picus, S. Hoyer, M. H. van Kerkwijk, M. Brett, A. Haldane, J. F. del Río, M. Wiebe, P. Peterson, P. Gérard-Marchant, K. Sheppard, T. Reddy, W. Weckesser, H. Abbasi, C. Gohlke, and T. E. Oliphant, Nature **585**, 357 (2020).

[36] S. K. Lam, A. Pitrou, and S. Seibert, in Proceedings of the second workshop on the llvm compiler infrastructure in hpc, LLVM '15 (2015).